Very Large Temperature-Induced Absorptive Loss in High Te-Containing Chalcogenide Fibers

Vinh Q. Nguyen, Jas S. Sanghera, Frederic H. Kung, Pablo C. Pureza, and Ishwar D. Aggarwal

***Abstract*—The change in the absorption loss relative to room temperature of the infrared (IR)-transmitting $Ge_{15}As_{35}Se_{(50-x)}Te_x$ glass fibers in the temperature range of $-110^{\circ}C \leq T \leq 110^{\circ}C$ was investigated. The attenuation increased significantly at $T \geq 40^{\circ}C$. This is mainly attributed to thermally activated free carriers associated with the semimetallic character of the Te atom. For $\lambda \leq 4.2$ μm, the loss due to electronic and free-carrier absorption was strongly affected by temperature. In the wavelength region of 5–11 μm, the loss was mainly due to free-carrier absorption. Beyond $\lambda \geq 11$ μm, multiphonon absorption dominated the loss spectrum at $T \leq 60^{\circ}C$ while free-carrier absorption contributed mainly to the total loss at $T \geq 80^{\circ}C$.**

***Index Terms*—Absorption loss, electronic, free-carrier, and multiphonon absorption, optical gap, tellurium (Te)-based glass fiber.**

I. Introduction

CHALCOGENIDE glasses are good candidates for applications in the infrared (IR) (1–13 μm) [1]. Chalcogenide glasses are vitreous materials which composed of mixtures of the chalcogen elements (Group IV): sulfur (S), selenium (Se), and tellurium (Te). The addition of the network formers (Group IV and V) such as silicon (Si), germanium (Ge), tin (Sn), phosphorus (P), arsenic (As), and antimony (Sb) establishes cross-linking between the tetrahedral and pyramidal units which facilitates stable glass formation [2]–[4]. Depending on the composition, the chalcogenide glasses are stable against crystallization, chemically inert, have excellent thermal stability, and are relatively easy to fiberize. Chalcogenide optical fibers are currently being used in laser power delivery (e.g., CO at 5.4 μm and CO_2 at 10.6 μm) as well as in fiber-optic chemical sensor systems using absorption, evanescent, and diffusive reflectance spectroscopy for environmental and Department of Defense (DOD) facility cleanup [5]–[8]. In addition, these fibers are used in IR countermeasure and laser threat warning systems to enhance aircraft survivability [9]. Other applications include temperature and pressure sensors as well as coherent IR image bundles. A thorough review of their applications is given by Sanghera *et al*. [10].

We have developed and fabricated stable low-loss IR-transmitting chalcogenide glass fibers which transmit to beyond 10 μm. Improved purification and processing techniques have been used to fabricate low-loss tellurium-containing fiber ($Ge_{30}As_{10}Se_{30}Te_{30}$) which transmits in the 2–10 μm region, with a minimum loss of 0.11 dB/m at 6.6 μm [11]. Similarly, arsenic-sulfide-based fibers ($As_{40}S_{(60-x)}Se_x$) which transmit in the 1–6.5 μm region, have been obtained with losses less than 0.1 dB/m in lengths of up to 50 m [12]. Since low-loss chalcogenide fibers are now enabling numerous applications, the question arises as to whether their loss is affected by environmental changes, especially temperature. In our previous work [13], we have investigated the effect of temperature on the absorption loss of the arsenic-sulfide-based fiber ($As_{40}S_{55}Se_5/As_{40}S_{60}$) and tellurium-containing fiber ($Ge_{30}As_{10}Se_{30}Te_{30}/Ge_{25}As_{12}Se_{40}Te_{23}$). However, the objective of this paper is to investigate the temperature dependence of the absorption loss in the IR-transmitting region for the high tellurium-based $Ge_{15}As_{35}Se_{(50-x)}Te_x$ glass fibers where $x =$ 35 and 40 at% Te. These high tellurium-containing glasses have lower phonon energies and are of interest for potential applications in the 8–12 μm wavelength region.

Manuscript received March 15, 2000; revised July 11, 2000.

V. Q. Nguyen, J. S. Sanghera, P. C. Pureza, and I. D. Aggarwal are with the Optical Science Division, Code 5606, Naval Research Laboratory, Washington, DC 20375 USA.

F. H. Kung is with the University of Maryland Research Foundation, Greenbelt, MD 20770 USA.

Publisher Item Identifier S 0733-8724(00)09100-3.

II. Experimental Methods

A. Fabrication of the High Tellurium-Based $Ge_{15}As_{35}Se_{(50-x)}Te_x$ Optical Fibers

Two compositions were selected for the high tellurium-based fiber, namely, $Ge_{15}As_{35}Se_{15}Te_{35}$ and $Ge_{15}As_{35}Se_{10}Te_{40}$. Higher concentrations of Te led to noticeable crystallization problems and so were not used in this study. The high tellurium-based fibers were made from high-purity glass rods. Commercially available six 9s purity of arsenic, selenium, and tellurium were baked out under dynamic vacuum (3×10^{-5} torr) at 450°C, 300°C, and 475°C, respectively, for 8 h to remove appropriate oxide impurities such as As_2O_3, As_2O_5, SeO_2, SeO_3, Se_2O_3, TeO, and TeO_3, respectively. Next, the arsenic, selenium, and tellurium were sublimed/distilled under dynamic vacuum at 500°C, 450°C, and 600°C to remove scattering centers such as carbon, quartz particles, residual trapped gases, and heavy transition elements. The three times zone-refined Ge was used as received.

High-quality quartz distillation ampoules were etched with 50/50 mol% of HF/deionized water for 3 min and then rinsed with deionized water several times. The ampoules were dried in a vacuum oven at 110°C for 8 h and then baked out under vacuum at elevated temperature (~900° C) using an oxygen–methane flame. Approximately 40-g batches of purified chemicals were batched in these ampoules inside a glove box under dry nitrogen atmosphere. These ampoules were evacuated at 2×10^{-5} torr for 5 h, sealed with an oxygen–methane torch, and placed in a two-zone furnace for melting. The melts

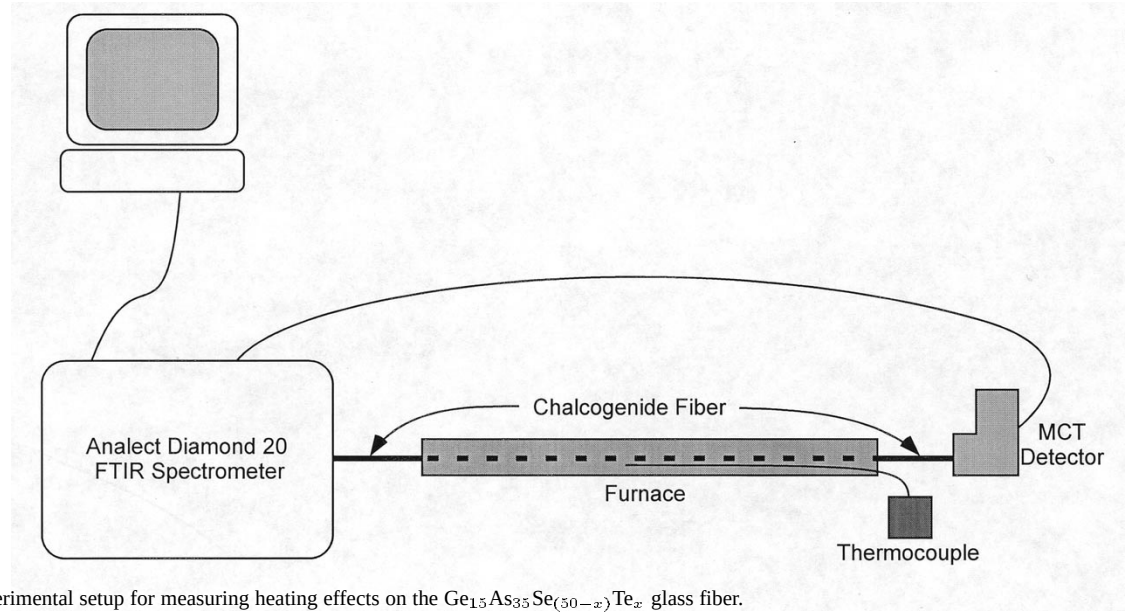

Fig. 1. Experimental setup for measuring heating effects on the $Ge_{15}As_{35}Se_{(50-x)}Te_x$ glass fiber.

were homogenized at 850°C for 10 h, distilled at 930°C for 8 h, and then remelted at 800°C for 20 h for homogeneity. Approximately 10 ppm of elemental Al was added to the initial batches to getter the oxygen impurities during melting prior to distillation. All the glass melts were quenched and annealed from the glass transition temperatures (180° C–200° C). Approximately 1-cm-diameter glass rods with lengths up to 6 cm were obtained. The $Ge_{15}As_{35}Se_{15}Te_{35}$ and $Ge_{15}As_{35}Se_{10}Te_{40}$ fibers were drawn at 355° C and 328° C, respectively, at a rate of 3–5 m/min depending on the required thickness of the fibers. In each case, the diameter of the uncoated fiber was 240 μm.

B. Experimental Setup of Heating and Cooling the Fibers

Fig. 1 shows the experimental setup used in the measurement of the relative change in transmission during heating with respect to room temperature. A 1-m-length fiber was placed inside a cylindrical furnace 75 cm long and 1.6 cm inner diameter. The temperature inside the furnace was controlled uniformly such that the change in temperature along the length of the furnace was ± 0.5°C. The two 12.5-cm end sections of the fiber outside the furnace were exposed to room temperature during the measurement. Fig. 2 shows the experimental setup used in the measurement of the relative change in transmission during cooling with respect to room temperature. Inside a styrofoam box, 2 m of fiber was placed on top of a 1/16–in-thick stainless-steel plate suspended above a liquid nitrogen bath. The atmosphere inside the styrofoam box was nitrogen. Two thermocouples were used to monitor the temperature. One was on the stainless-steel plate and the other was about 2 mm above the stainless-steel plate. The temperature readings from these two thermocouples were within ± 1°C. To achieve thermal equilibrium, during heating and cooling the temperature inside the furnace and styrofoam box was held approximately constant for 15 min before each measurement was made.

C. Fiber Characterization

The fiber optical attenuation at room temperature was characterized using a FTIR spectrometer (Analect Diamond 20) and standard cutback technique [14]. The light source was a broad-band NiCr wire and the detector was a liquid-nitrogen-cooled MCT detector. While the spectrometer operated between 1.3 and 24 μm, only the data between 3.5 and 12.0 μm was reported. The fiber attenuation (dB/m) was determined from the following relationship:

$$\text{Attenuation (dB/m)} = \frac{10\log_{10}(P_o/P)}{L - L_o} \tag{1}$$

where P_o and P are the measured powers at a given wavelength for the cutback length and the long length, respectively, and L and L_o are the length of the fiber and the cutback section, respectively.

The relative change in transmission of a fiber due to varying temperature was determined using the following method. The ends of the fiber were connected to the FTIR spectrometer. The intensity of the light transmitted through the fiber at room temperature $[I_o]$ was recorded and this was used as the reference for the measurement. The intensity $[I_T]$ of the transmitted light was recorded at specific temperatures (10°C increments above or below room temperature) as the fiber was either heated or cooled. The relative change in loss was calculated by the following equation:

$$\text{Relative } \Delta\text{Loss (dB/m)} = \pm\frac{10}{l} \times \log_{10}[\Delta\text{Trans}] \tag{2}$$

where the plus sign $(+)$ is for heating, and the minus sign $(-)$ is for cooling, l is the length of the fiber in the heating/cooling zone, and $\Delta\text{Trans} = I_T/I_o$. We have repeated the experiment three times using the same fiber and the data did not change. This seems to indicate that the loss is reversible between the temperature range in this study.

D. Measurement of the Optical Gap

The absorption spectra near the electronic edge were measured using a Cary 5G spectrophotometer on 3-mm-thick samples with an optical finish on both end faces. The absorption data was normalized with respect to the sample's thickness.

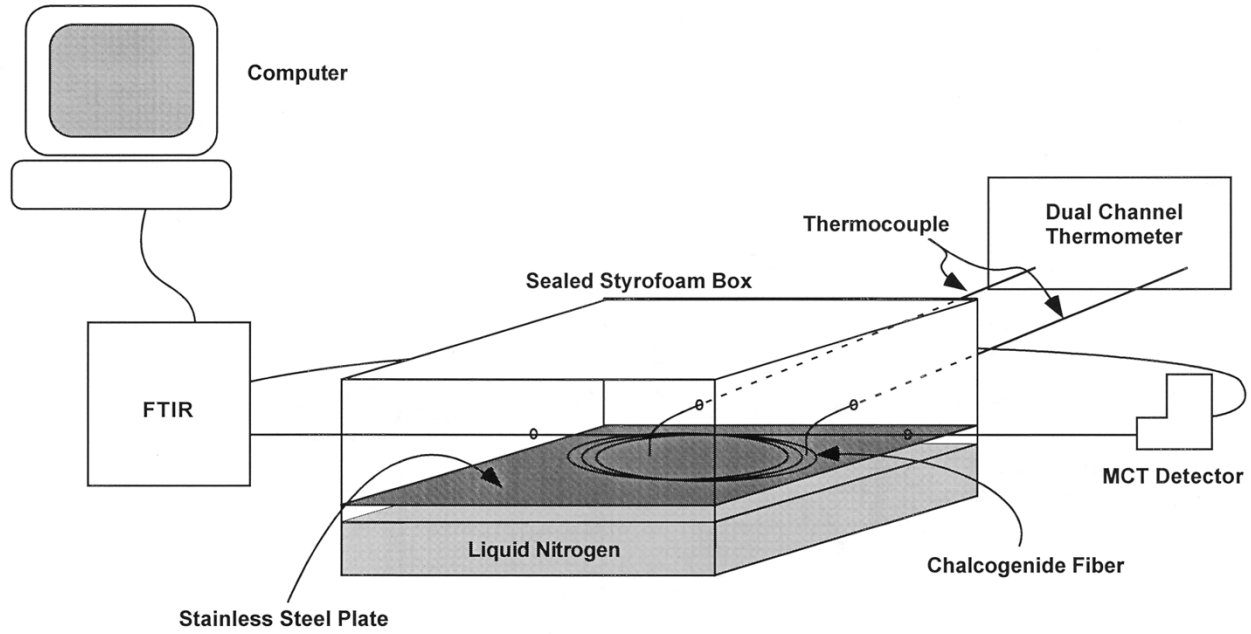

Fig. 2. Experimental setup for measuring cooling effects on the $Ge_{15}As_{35}Se_{(50-x)}Te_x$ glass fiber.

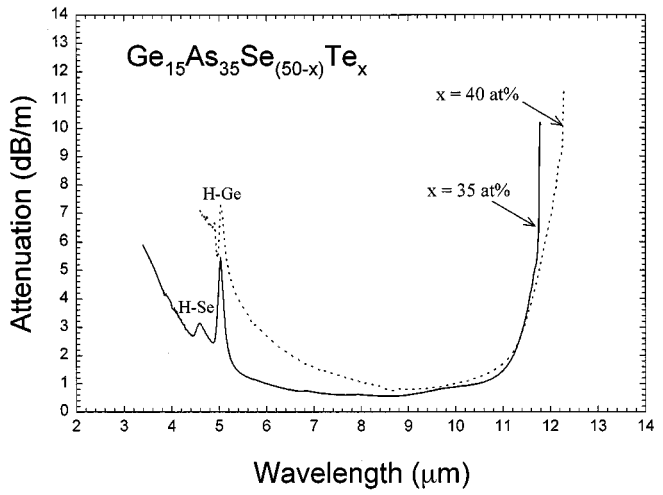

Fig. 3. The attenuation versus wavelength plot for unclad $Ge_{15}As_{35}Se_{15}Te_{35}$ and $Ge_{15}As_{35}Se_{10}Te_{40}$ glass fiber. The optical loss was measured on a 2-m fiber length with a 1-m length cutback.

III. Results and Discussion

A. Fiber Attenuation

Fig. 3 shows the measured attenuation at room temperature for the $Ge_{15}As_{35}Se_{(50-x)}Te_x$ glass fibers. The minimum losses of the x =35- and 40-at% composition are 0.56 dB/m at 8.70 μm and 0.74 dB/m at 8.63 μm, respectively. There are two major bands at 4.55 and 5.0 μm which are attributed to the H–Se stretching vibration [15] and H–Ge stretching vibration [16], respectively. The sources of hydrogen impurities are mainly from the germanium since the germanium was used as-received and from the residual hydrogen impurities in the As, Se, and Te chemicals. At 10.6 μm, the attenuations of the fiber for x =35- and 40-at% composition are 1.00 and 1.34 dB/m, respectively. These are the lowest losses reported to-date for any chalcogenide glasses at 10.6 μm. For the $Ge_{15}As_{35}Se_{15}Te_{35}$ composition, the fiber exhibits less than 1-dB/m loss in the region between 6.0 and 10.6 μm. The increase in the Te content shifts both the electronic and multiphonon edges to longer wavelengths. The shift in the electronic edge leads to a smaller energy gap thereby enhancing electronic absorptions. The shift in the multiphonon edge results from the larger reduced mass and weaker semimetallic bonding character of the Te atom.

B. Optical Gap

The fundamental optical gap of chalcogenide glasses can be determined from the spectral dependence of $\alpha(h\nu)$ via Tauc's relationship [17]

$$(\alpha h\nu)^{1/2} = B(h\nu - E_o) \tag{3}$$

where

- α absorption coefficient (cm^{-1});
- h Planck's constant (eV·s);
- ν frequency (s^{-1});
- B material-dependent constant;
- E_o optical gap (eV).

The intercept of $(\alpha h\nu)^{1/2}$ versus $h\nu$ yields the value of the optical gap. Fig. 4 shows the plot of $(\alpha h\nu)^{1/2}$ as a function of photon energy $(h\nu)$ for the two glasses measured at room temperature. The measured values of the optical gap for the $Ge_{15}As_{35}Se_{15}Te_{35}$ and $Ge_{15}As_{35}Se_{10}Te_{40}$ glasses are 0.98 and 0.90 eV, respectively. The lowering of the optical gap by increasing tellurium content has been attributed to the broadening of the valence and conduction bands into the energy gap [18].

C. Heating of the Glass Fiber ($110°C \geq T \geq 20°C$)

Fig. 5(a) and (b) shows the attenuation of the $Ge_{15}As_{35}Se_{15}Te_{35}$ and $Ge_{15}As_{35}Se_{10}Te_{40}$ glass fiber as temperature is increased from 20°C to 110°C, respectively.

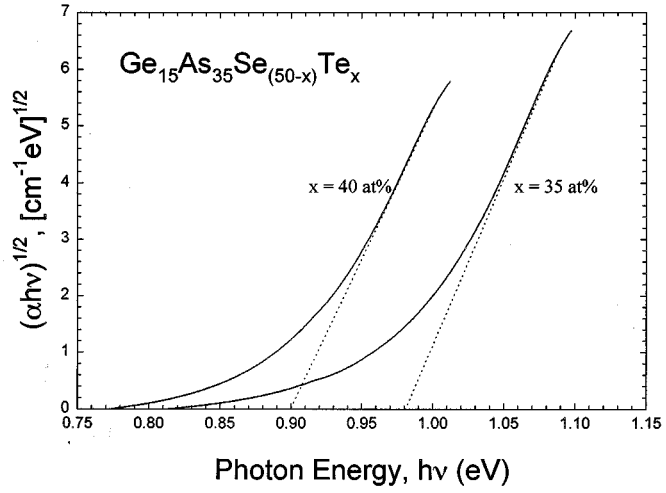

Fig. 4. Determination of the optical gap—$(\alpha h\nu)^{1/2}$ as a function of photon energy $(h\nu)$.

In the short-wavelength cutoff region ($\lambda \leq 4.1\,\mu$m), the loss curve follows the standard Urbach edge [19] behavior which occurs when free electrons in the mobility edge absorb sufficient photon energy and jump across the optical gap into the conduction band. The loss $(\Delta\alpha_{\rm el})$ increases with higher temperature in accordance with the following empirical relationship:

$$\Delta\alpha_{\rm el} = C(T)\exp(d(T)/\lambda) - C\exp(d/\lambda) \tag{4}$$

where $C(T)\exp(d(T)/\lambda)$ is the electronic absorption at temperature T and $C\exp(d/\lambda)$ is the electronic absorption at room temperature; $C(T)$ and $d(T)$ are material and temperature-dependent constants.

In the $Ge_{15}As_{35}Se_{(50-x)}Te_x$ tellurium-based glass, since tellurium possesses semimetallic character, the free-electron concentration increases with temperature because of the smaller optical gap ($E_o = 0.90$–0.98 eV). Depending on the temperature, this free-electron concentration would contribute to the overall loss spectrum as free-carrier absorption. The free-carrier absorption is an indirect process which involves both a photon and phonon. This occurs when electrons in the lower conduction band absorb the incident electromagnetic radiation and are excited to the higher lying conduction bands (intraband absorption) or states in different bands (interband absorption). As temperature increases, these electrons are scattered inelastically by lattice vibrations, transferring energy to the lattice of the material. The free-carrier absorption $(\alpha_{\rm fc})$ follows the empirical relationship [20], [21]

$$\alpha_{\rm fc}(T) = G\lambda^m + G_o\exp(-E_o/k_BT) \tag{5}$$

where the first and second terms in (5) represent the intraband and interband absorption, respectively. G is the constant for optical phonon scattering, m lies between $1.5 \leq m \leq 3.5$,, G_o is the material constant, E_o is the optical energy, k_B is the Boltzmann constant, and T is the temperature. Free carrier absorption is enhanced by high temperature and by materials which possess a larger carrier mobility (m) value. The absorption depends upon the free-carrier concentration which obeys Fermi statistics.

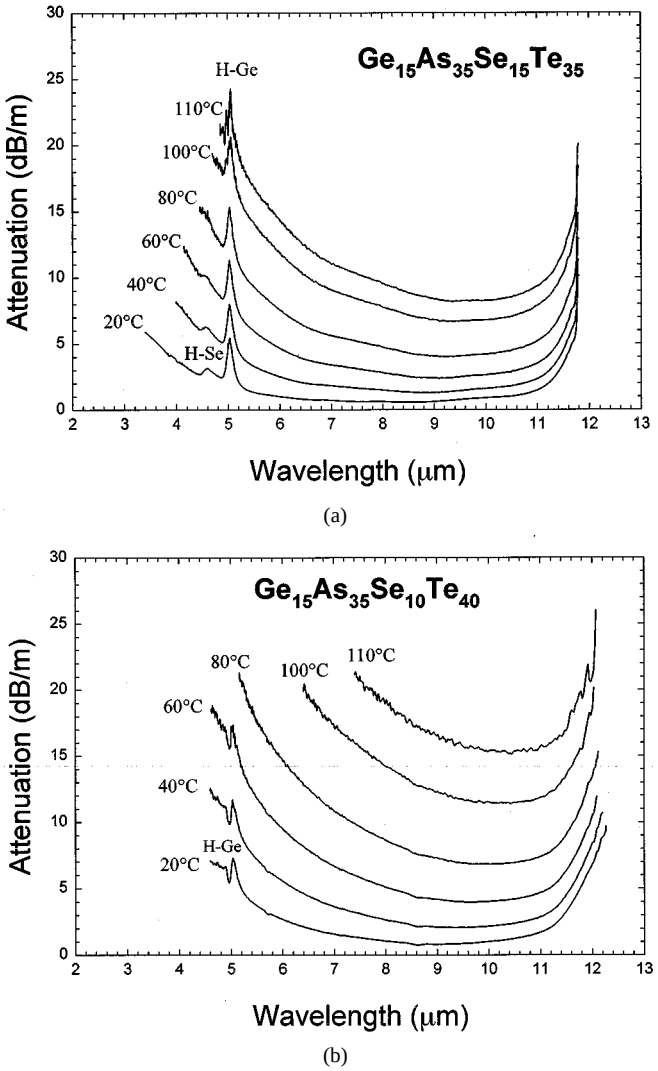

Fig. 5. Effect of heating on the change in loss of (a) $Ge_{15}As_{35}Se_{15}Te_{35}$ and (b) $Ge_{15}As_{35}Se_{10}Te_{40}$ glass fiber. The length of the fiber used in the heating experiment is 1 m.

From Fig. 5(a) and (b) at $T \geq 30^\circ$C in the electronic edge region ($\lambda \leq 4.1\ \mu$m), the attenuation is due to both electronic and free-carrier absorption, i.e., $\alpha(T) = \alpha_{\rm el}(T) + \alpha_{\rm fc}(T)$. At $T = 30^\circ$C, the attenuation is predominantly due to electronic absorption, whereas at $T = 110^\circ$C, both the electronic and free-carrier absorption contributed to the total loss. At high temperature ($T = 110^\circ$C) the loss is large such that the optical transparency of the fiber disappears in the region of $\lambda \leq 4.1\,\mu$m.

Between the electronic and multiphonon edges ($5\ \mu$m $\leq \lambda \leq 11\ \mu$m), the attenuation is due mainly to free-carrier absorption, wavelength-independent scattering, and Rayleigh scattering. Rayleigh scattering $(\alpha_{\rm RS})$ occurs due to compositional and density fluctuations in the material on a microscopic level, which leads to localized changes in the dielectric constant. This fluctuation in the dielectric constant and variation in the refractive index lead to Rayleigh scattering $(C_{\rm RS}/\lambda^{-4})$ where $C_{\rm RS}$ is the Rayleigh scattering coefficient [22]. In our previous work [13], we have determined the change in Rayleigh scattering loss with respect to temperature $d(\alpha_{\rm RS})/dT$ in the Ge–As–Se–Te glass system is negligible ($<10^{-8}$ dB). Wave-

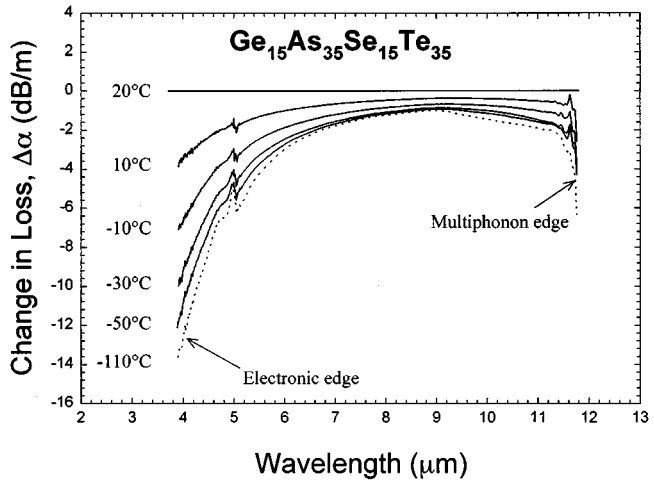

(a)

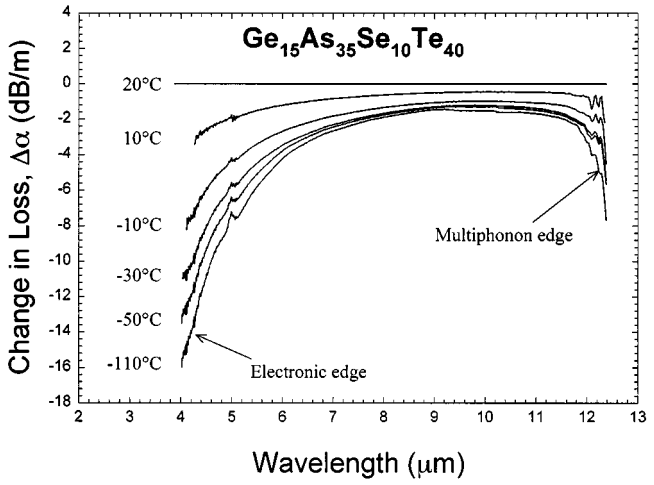

(b)

Fig. 6. Effect of cooling on the change in loss of (a) $Ge_{15}As_{35}Se_{15}Te_{35}$ and (b) $Ge_{15}As_{35}Se_{10}Te_{40}$ glass fiber. The length of the fiber used in the cooling experiment is 2 m.

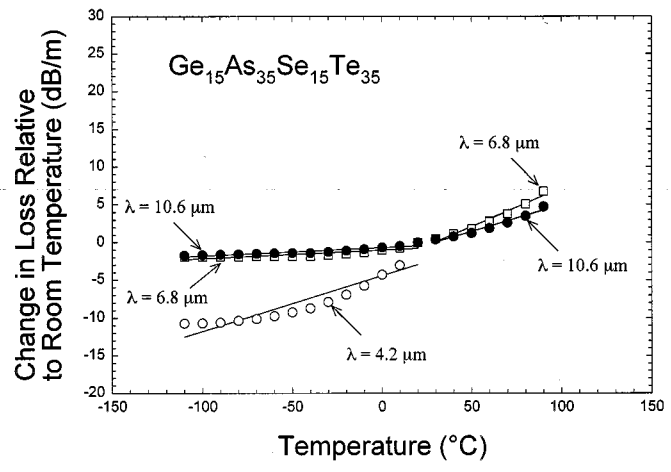

(a)

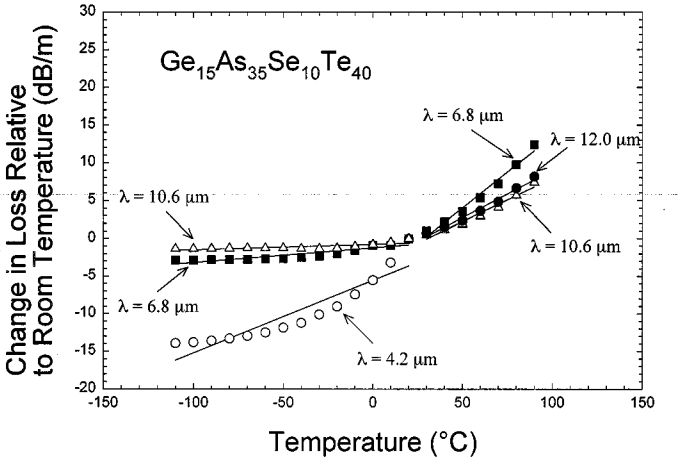

(b)

Fig. 7. Change in loss of (a) $Ge_{15}As_{35}Se_{15}Te_{35}$ and (b) $Ge_{15}As_{35}Se_{10}Te_{40}$ glass fiber as a function of temperature at distinct wavelengths.

length-independent scattering is not expected to change noticeably with temperature. Therefore, at high temperature the increased change in loss between 5 and 11 μm is mainly due to free-carrier absorption [see (5)].

Fig. 3 shows that beyond 11 μm, multiphonon absorption takes place. The multiphonon absorption is directly due to nonlinearities in the electric dipole moment [23], and indirectly from anharmonic interaction between IR-active phonons and photons [24]. Anharmonic interaction occurs since the number of phonons increase with temperature in accordance with the Planck distribution function $\langle n\rangle = \{\exp(\hbar\omega/kT)-1\}^{-1}$. The multiphonon absorption increases with higher temperature in accordance to the following relation:

$$\Delta\alpha_{\rm mp} = A(T)\exp(b(T)\lambda) - A\exp(b\lambda) \tag{6}$$

where $A(T)\exp(b(T)\lambda)$ is the multiphonon absorption at temperature T and $A\exp(b\lambda)$ is the multiphonon absorption at room temperature. $A(T)$ and $b(T)$ are material and temperature dependent constants, and λ is the wavelength. Thus from Fig. 5(a) and (b) at temperature $T = 110^{\circ}$C and $\lambda \geq 11$ μm, the attenuation associated with the long-wavelength absorption edge is due to free-carrier absorption and multiphonon absorption $(\alpha_{\rm mp})$, i.e., $\alpha(T) = \alpha_{\rm fc}(T) + \alpha_{\rm mp}(T)$. Inagawa *et al.* [25] have shown that for the Ge–As–Se–Te glass system the activation energies for the multiphonon and free-carrier absorption are 0.06 eV (23–67°C) and 0.01 eV (77–127°C), respectively. Fig. 5(a) and (b) shows that for the $Ge_{15}As_{35}Se_{15}Te_{35}$ and $Ge_{15}As_{35}Se_{10}Te_{40}$ fibers the dominant loss mechanism is due to free-carrier absorption at $T \geq 30^{\circ}$C. It is also apparent that the free-carrier absorption is larger in the higher Te-containing fiber. The change in the multiphonon absorption with temperature in the 11–12 μm region does not appear to increase as significantly as the free-carrier absorption. At 110°C and 10 μm, the increase in loss is about 15 dB/m relative to 20°C and is attributed predominantly to free-carrier absorption. The increase in the multiphonon edge at about 12 μm is approximately 23 dB/m of which 15 dB/m is attributed to free carrier absorption [Fig. 5(b)]. Therefore, the increase in the multiphonon absorption is only about 7 dB/m.

D. Cooling of the Glass Fiber ($20^{\circ}C \geq T \geq -110^{\circ}C$)

Since a different length of the fiber was used for the cooling experiment and we did not measure the fiber attenuation, the loss of the fiber might be higher than the fiber section used for

TABLE I
TEMPERATURE DEPENDENCE OF THE CHANGE IN LOSS OF THE $Ge_{15}As_{35}Se_{(50-x)}Te_x$ GLASSES

Fiber	λ (μm)	d(△α)/dT (dB/m/°C)	
		90°C ≥T ≥20°C	20°C ≥T ≥-110°C
$Ge_{15}As_{35}Se_{15}Te_{35}$	4.2	--	7.4 x 10^{-2}
	6.8	1.0 x 10^{-1}	1.2 x 10^{-1}
	10.6	7.1 x 10^{-2}	1.1 x 10^{-1}
	12.0	-	-
$Ge_{15}As_{35}Se_{10}Te_{40}$	4.2	--	9.7 x 10^{-2}
	6.8	1.9 x 10^{-1}	2.0 x 10^{-1}
	10.6	1.1 x 10^{-1}	7.3 x 10^{-3}
	12.0	1.2 x 10^{-1}	2.0 x 10^{-2}

the heating experiment. Therefore, the effect of temperature on cooling will be represent as change in loss with respect to temperature. Fig. 6(a) and (b) shows the change in loss of the $Ge_{15}As_{35}Se_{15}Te_{35}$ and $Ge_{15}As_{35}Se_{10}Te_{40}$ glass fibers as temperature decreased from 20°C to −110°C, respectively. The band at 5.0 μm is due to the stretching vibration of H–Ge [16]. For the Urbach edge region ($\lambda \leq 4.1$ μm) the loss decreases and is due to less thermally activated free electrons in the mobility edge able to jump across the gap into the conduction band. Also, since the tellurium-based $Ge_{15}As_{35}Se_{(50-x)}Te_x$ glass possesses semimetallic character, the optical gap widens as temperature decreases and the excitation of free electrons in the mobility edge and excitation of bound valence electrons into the conduction band becomes less likely. Between the short- and long-wavelength region (8–11 μm), the overall change in loss is relatively small, i.e., the effect of free-carrier absorption is small since free carriers are thermally activated. Beyond 11 μm, the $Ge_{15}As_{35}Se_{15}Te_{35}$ and $Ge_{15}As_{35}Se_{10}Te_{40}$ glass fibers become more transparent with cooling due to reduced multiphonon and free-carrier absorption. This is due to less anharmonic interaction since the number of phonons $\langle n \rangle$ available is lower. Perhaps slightly larger decrease in loss in the 6–11 μm region for the 40 at% Te fiber is due to initially more free carrier absorption at 20°C.

E. Determination of Temperature Dependence of the Change in Loss $d(\Delta\alpha)/dT$

Fig. 7(a) and (b) shows the change in loss relative to room temperature of the $Ge_{15}As_{35}Se_{15}Te_{35}$ and $Ge_{15}As_{35}Se_{10}Te_{40}$ glass fibers at four distinct wavelengths, namely, at 4.2, 6.8, 10.6, and 12.0 μm. At the electronic edge region ($\lambda = 4.2$ μm), for $20°C \geq T \geq -110°C$ a larger slope in the change in loss relative to room temperature was observed compared to $\lambda = 6.8$ and 10.6 μm. As stated in previous paragraphs, electronic and free-carrier absorption contribute to the total loss for $\lambda \leq 4.2$ μm. As temperature decreases, the optical gap widens and the free carriers become less thermally activated. Therefore, electronic and free-carrier absorptions become less easily to occur. This results in a larger slope in the change in loss relative to room temperature.

From Fig. 7(a) and (b), at 6.8 and 10.6 μm for temperatures between −110°C and 20°C, there is only a small increase in the loss relative to room temperature. At temperatures between 20°C and 90°C, there is a larger increase in the loss relative to room temperature. For comparison, at 6.8 and 10.6 μm, the $Ge_{15}As_{35}Se_{10}Te_{40}$ glass fiber [Fig. 7(b)] has a larger increase in loss than the $Ge_{15}As_{35}Se_{15}Te_{35}$ glass fiber [Fig. 7(a)]. This is due to a higher free-carrier absorption associated with higher free-electron concentration in the $Ge_{15}As_{35}Se_{10}Te_{40}$ glass fiber.

From Fig. 7(b) at the multiphonon edge region ($\lambda = 12.0$ μm), at temperature between −110°C and 20°C, there is a small increase in the loss relative to room temperature, i.e., the data for $\lambda = 12.0$ μm lies between $\lambda = 6.8$ and 10.6 μm and will be left out for clarity. Between 20°C and 90°C, there is a larger increase in the loss relative to room temperature, comparable to the change in loss for $\lambda = 6.8$ and 10.6 μm. This is attributed to the significantly higher contribution from free-carrier absorption with rising temperature. From Fig. 7(a) and (b), by using linear regression, the temperature dependence

of the change in loss $d(\Delta\alpha)/dT$ of the $Ge_{15}As_{35}Se_{15}Te_{35}$ and $Ge_{15}As_{35}Se_{10}Te_{40}$ glass fibers at λ =4.2, 6.8, 10.6, and 12.0μm was calculated and listed in Table I.

Table I indicates that at 4.2 and 6.8 μm, the $Ge_{15}As_{35}Se_{10}Te_{40}$ glass fiber has a larger $d(\Delta\alpha)/dT$ com- pared to the $Ge_{15}As_{35}Se_{15}Te_{35}$ glass fiber. This is attributed to the higher free-carrier absorption due to the larger free-electron concentration associated with the Te atom. At 10.6 μm and between 20°C $\geq T \geq -$110°C, the $Ge_{15}As_{35}Se_{10}Te_{40}$ glass fiber has a smaller $d(\Delta\alpha)/dT$ than the $Ge_{15}As_{35}Se_{15}Te_{35}$ glass fiber. This is due to the shifting of the multiphonon edge to longer wavelength thereby reducing the contribution of multiphonon absorption. However, at 10.6 μm and between 90°C $\geq T \geq$ 20°C, the $Ge_{15}As_{35}Se_{10}Te_{40}$ glass fiber has a slight larger $d(\Delta\alpha)/dT$ compared to the $Ge_{15}As_{35}Se_{15}Te_{35}$ glass fiber. This is primarily related to the higher free-carrier absorption.

At higher temperatures $T \geq$ 60°C, the losses increase significantly over the entire wavelength range, but especially at short and long wavelengths. This makes potential applications difficult. However, at temperatures $T \leq$ 30°C, the high tellurium-containing fibers can be used in relatively short lengths in the wavelength region of about 5–12 μm.

IV. Summary

The attenuation of the $Ge_{15}As_{35}Se_{(50-x)}Te_x$ glass fiber as a function of temperature has been investigated. The smaller optical gap and the larger free-electron concentration possessed by the $Ge_{15}As_{35}Se_{10}Te_{40}$ glass fiber makes it possible for thermally activated free electrons to be excited from the valence to the conduction band and increases the loss in the region of the electronic absorption edge ($\lambda \leq$ 4.2 μm). Between the wavelengths of 5 and 11 μm, the $Ge_{15}As_{35}Se_{(50-x)}Te_x$ glass fibers exhibit a large free-carrier absorption above 30°C. The long-wavelength edge ($\lambda \geq$ 11 μm) is dominated by free-carrier absorption at $T \geq$ 30°C.

References

[1] J. R. Gannon, "Materials for mid-infrared waveguides," *SPIE*, vol. 266, pp. 62–68, Feb. 1981.

[2] G. Lucovsky and R. M. Martin, "A molecular model for the vibrational modes in chalcogenide glasses," *J. Non-Cryst. Solids*, vol. 8–10, pp. 185–190, 1972.

[3] G. J. Ball and J. M. Chamberlain, "Infrared structural studies of Ge_ySe_{1-y} glasses," *J. Non-Cryst. Solids*, vol. 29, pp. 239–248, July 1978.

[4] V. Q. Nguyen, J. S. Sanghera, J. A. Freitas, I. D. Aggarwal, and I. K. Lloyd, "Structural investigations of chalcogenide and chalcohalide glasses using Raman spectroscopy," *J. Non-Cryst. Solids*, vol. 248, no. 2–3, pp. 103–114, June 1999.

[5] J. S. Sanghera, F. H. Kung, L. E. Busse, P. C. Pureza, and I. D. Aggarwal, "Infrared evanescent absorption spectroscopy of toxic chemicals using chalcogenide glass fibers," *J. Amer. Ceram. Soc.*, vol. 78, no. 8, pp. 2198–2202, Aug. 1995.

[6] G. Nau, F. Bucholtz, K. J. Ewing, S. T. Vohra, J. S. Sanghera, and I. D. Aggarwal, "Fiber optic IR reflectance sensor for the cone penetrometer," *SPIE*, vol. 2504, pp. 291–296, June 1995.

[7] L. E. Busse, J. S. Sanghera, and I. D. Aggarwal, "High optical power transmission through glass cladded infrared fiber," in *Proc. 1994 IRIS Specialty Group Infrared Materials*. Ann Arbor, MI: Erim, May 1995, pp. 341–346.

[8] J. S. Sanghera, I. D. Aggarwal, L. E. Busse, P. C. Pureza, V. Q. Nguyen, R. Miklos, F. H. Kung, and R. Mossadegh, "Development of low loss IR transmitting chalcogenide glass fibers," *SPIE*, vol. 2396, pp. 71–77, Feb. 1995.

[9] L. E. Busse, J. Moon, J. S. Sanghera, and I. D. Aggarwal, "Chalcogenide fibers deliver high IR power," *Laser World Focus*, vol. 32, no. 9, pp. 143–150, Sept. 1996.

[10] J. S. Sanghera and I. D. Aggarwal, "Active and passive chalcogenide glass optical fibers for IR applications: A review," *J. Non-Cryst. Solids*, vol. 256 \257, pp. 6–16, Oct. 1999.

[11] J. S. Sanghera, V. Q. Nguyen, P. C. Pureza, F. H. Kung, R. Miklos, and I. D. Aggarwal, "Fabrication of low-loss IR-transmitting $Ge_{30}As_{10}Se_{30}Te_{30}$ glass fibers," *J. Lightwave Technol.*, vol. 12, pp. 737–741, May 1994.

[12] J. S. Sanghera, V. Q. Nguyen, P. C. Pureza, R. Miklos, F. H. Kung, and I. D. Aggarwal, "Fabrication of long lengths of low-loss IR transmitting $As_{40}S_{(60-x)}Se_x$ glass fibers," *J. Lightwave Technol.*, vol. 14, pp. 743–748, May 1996.

[13] V. Q. Nguyen, J. S. Sanghera, F. H. Kung, I. D. Aggarwal, and I. K. Lloyd, "Effect of temperature on the absorption loss of chalcogenide optical fibers," *Appl. Opt.*, vol. 38, no. 15, pp. 3206–3213, May 1999.

[14] R. D. Driver, G. M. Leskowitz, L. E. Curtiss, D. E. Moynihan, and L. B. Vacha, "The characterization of infrared transmitting optical fibers," *Proc. Materials Research Soc. Symp.*, vol. 172, pp. 169–175, Jan. 1990.

[15] C. T. Moynihan, P. B. Macedo, M. S. Maklad, R. K. Mohr, and R. E. Howard, "Intrinsic and impurity infrared absorption in As_2Se_3 glass," *J. Non-Cryst. Solids*, vol. 17, pp. 369–385, 1975.

[16] G. G. Devyatykh, M. F. Churbanov, I. V. Scripachev, E. M. Dianov, and V. G. Plotnichenko, "Middle infrared As-S, As-Se, Ge-As-Se chalcogenide glass fibers," *Int. J. Optoelectron.*, vol. 7, no. 2, pp. 237–254, Mar. 1992.

[17] J. Tauc, R. Grigorovici, and A. Vancu, "Optical properties of electronic structure of amorphous germanium," *Phys. Status Solidi*, vol. 15, pp. 627–637, 1966.

[18] V. Q. Nguyen, J. S. Sanghera, I. D. Aggarwal, and I. K. Lloyd, "Optical properties of chalcogenide glasses," *J. Non-Cryst. Solids*, submitted for publication.

[19] F. Urbach, "The long-wavelength edge of photographic sensitivity and of the electronic absorption of solids," *Phys. Rev.*, vol. 92, no. 5, pp. 1324–1325, Dec. 1953.

[20] J. I. Pankove, *Optical Processes in Semiconductors*. New York: Dover, 1971, p. 74.

[21] R. H. Bube, *Electrons in Solids*, 3rd ed. New York: Academic, 1992, pp. 134–141.

[22] R. Olshansky, "Propagation in glass optical waveguides," *Rev. Mod. Phys.*, vol. 51, no. 2, pp. 341–368, Apr. 1979.

[23] M. Lax and E. Burstein, "Infrared lattice absorption in ionic and homopolar crystals," *Phys. Rev.*, vol. 97, no. 1, pp. 39–52, Jan. 1955.

[24] M. Born and K. Huang, *Dynamical Theory of Crystal Lattices*. New York, London: Oxford Univ. Press, 1954, pp. 38–116.

[25] I. Inagawa, S. Moromoto, T. Yamashita, and I. Shirotani, "Temperature dependence of transmission loss of chalcogenide glass fibers," *Japan J. Appl. Phys.*, vol. 36, pp. 2229–2235, Apr. 1997.

Vinh Q. Nguyen, photograph and biography not available at the time of publication.

Jas S. Sanghera, photograph and biography not available at the time of publication.

Frederic H. Kung, photograph and biography not available at the time of publication.

Pablo C. Pureza, photograph and biography not available at the time of publication.

Ishwar D. Aggarwal, photograph and biography not available at the time of publication.